

Electronic Supplementary Information (ESI)

**Crystal structure control of RuCuRhIrPt high-entropy alloy  
nanoparticles with a face-centered cubic or hexagonal close-packed  
phase**

*Weiyang Yang<sup>a</sup>, Maiyong Zhu<sup>\*d</sup> and Quan Zhang<sup>\*abc</sup>*

*<sup>a</sup> State Key Laboratory of Advanced Fiber Materials, College of Materials Science and Engineering, Donghua University, Shanghai 201620, China.*

*<sup>b</sup> Dishui Lake laboratory, Shanghai Dianji University, Shanghai 201306, China.*

*<sup>c</sup> State Key Laboratory of Structural Chemistry, Fujian Institute of Research on the Structure of Matter, Chinese Academy of Sciences, Fuzhou, 350002, China.*

*<sup>d</sup> School of Materials Science & Engineering, Jiangsu University, Zhenjiang, 212013, China*

*\* Corresponding authors*

*E-mail: maiyongzhu@ujs.edu.cn; zhangquan@dhu.edu.cn*

## Experiment

### Materials

Triethylene glycol (TEG), Diethylene glycol (DEG), poly(N-vinyl-2-pyrrolidone) (PVP, K30, MW  $\approx$  40000), ruthenium(III) acetylacetonate ( $\text{Ru}(\text{acac})_3$ ), hexachloroplatinic(IV) acid hexahydrate ( $\text{H}_2\text{PtCl}_6 \cdot 6\text{H}_2\text{O}$ ) were purchased from Aladdin (Shanghai, China). Hydrogen hexachloroiridate(IV) hydrate ( $\text{H}_2\text{IrCl}_6 \cdot x\text{H}_2\text{O}$ ), rhodium(III) chloride trihydrate ( $\text{RhCl}_3 \cdot 3\text{H}_2\text{O}$ ), copper(II) acetate monohydrate ( $\text{C}_4\text{H}_6\text{CuO}_4 \cdot \text{H}_2\text{O}$ ), ruthenium(III) chloride hydrate ( $\text{RuCl}_3 \cdot x\text{H}_2\text{O}$ ) were purchased from Sinopharm Chemical Reagent Co., Ltd (Shanghai, China). 5 wt% Nafion solution and 20 wt% Pt/C catalyst was purchased from Sigma-Aldrich and Johnson Matthey, respectively.

### Synthesis of fcc-RuCuRhIrPt/C NPs

Typically, PVP (4 mmol, 444 mg) was dissolved in 100 mL of DEG and the solution was heated to 190 °C. Separately, the five metal precursors—  $\text{Ru}(\text{acac})_3$  (0.28 mmol),  $\text{H}_2\text{PtCl}_6 \cdot 6\text{H}_2\text{O}$  (0.03 mmol),  $\text{H}_2\text{IrCl}_6 \cdot x\text{H}_2\text{O}$  (0.03 mmol),  $\text{RhCl}_3 \cdot 3\text{H}_2\text{O}$  (0.03 mmol) and  $\text{C}_4\text{H}_6\text{CuO}_4 \cdot \text{H}_2\text{O}$  (0.03 mmol)— were dissolved in 50 mL of DEG. The resulting precursor solution was dropped into the preheated TEG/PVP solution at a rate of 1 mL  $\text{min}^{-1}$ . After the complete addition of the precursor solution, the mixture was kept at 190 °C for 10 min and then cool to room temperature. The resulting HEA NPs were collected by centrifugation using diethyl ether and acetone, and the obtained black powder was uniformly dispersed on carbon black (VULCAN XC-72R) to obtain fcc-RuCuRhIrPt/C with a metal loading of 20 wt%.

### Synthesis of hcp-RuCuRhIrPt/C NPs

To obtain the hcp RuCuRhIrPt/C NPs, the as-synthesized fcc-RuCuRhIrPt/C was sealed under 100 kPa of  $\text{H}_2$  and annealed at 300 °C for 0.5 h. The resulting black powders were then collected.

### Synthesis of hcp-Ru NPs

Typically, 0.4 mmol  $\text{RuCl}_3 \cdot x\text{H}_2\text{O}$  was dissolved in 100 mL TEG with 4 mmol PVP. The mixture was then heated to 200 °C and stirred magnetically for 0.5 h.

Finally, the resulting black powder was collected by centrifugation using diethyl ether and acetone.

### **General Characterization**

Powder X-ray diffraction (PXRD) was conducted with a Rigaku Ultima IV diffractometer equipped with a Cu K $\alpha$  radiation source ( $\lambda = 1.5418 \text{ \AA}$ ). Rietveld refinements were performed using the TOPAS3 software (Bruker AXS GmbH, Karlsruhe, Germany). Elemental compositions were determined by inductively coupled plasma-optical emission spectroscopy (ICP-OES) on a Leeman Prodigy spectrometer (Leeman Labs, USA). HAADF-STEM images were obtained on an aberration-corrected transmission electron microscope (JEOL ARM-300F, JEOL Ltd., Japan) operated at 300 kV. X-ray photoelectron spectroscopy (XPS) results were obtained with a Thermo Scientific ESCALAB 250Xi spectrometer. All measured values of the electron binding energy were calibrated with respect to the principal peak of C 1s at 284.8 eV as the internal standard.

### **Electrochemical measurements**

The hydrogen evolution reaction (HER) was carried out at room temperature in 1.0 M KOH using an electrochemical workstation (CHI760E, CH Instruments, USA) with a three-electrode configuration: rotating disk working electrode, Hg/HgO reference electrode, and graphite rod counter electrode. The catalyst inks were prepared by dispersing the carbon-supported sample in a mixture of isopropanol (0.6 mL), water (0.3 mL), and 5 wt% Nafion solution (0.1 mL). The working electrodes were fabricated by drop 10  $\mu\text{L}$  of the catalyst ink (0.05 mg metal  $\text{cm}^{-2}$ ) onto a glassy carbon electrode (5 mm diameter, 0.196  $\text{cm}^2$ ) and air dried overnight. Prior to catalyst deposition, the glassy carbon surfaces were polished with diamond and alumina suspensions.

The working electrodes were initially activated in Ar-saturated 1.0 M KOH between -0.85 and 0.2 V (vs. Hg/HgO) at 200  $\text{mV s}^{-1}$  for several hundred cycles. The HER activity was assessed using linear sweep voltammetry at a rotation rate of 1600 rpm and a scan rate of 5  $\text{mV s}^{-1}$ . The catalyst durability was evaluated by chronopotentiometry for 12 h. All polarization curves were iR-corrected with an 80%

solution resistance compensation.

### Electrochemical surface area

The number of active sites ( $n$ ) and turnover frequency (TOF) were derived from the ECSA measured by Cu UPD.<sup>1-3</sup> To obtain ECSA, the electrodes were cycled several hundred times between 0.05 and 1.05 V at 500 mV s<sup>-1</sup> in Ar-saturated 0.5 M H<sub>2</sub>SO<sub>4</sub>, followed by holding at -0.02 V for 2 min to eliminate surface oxides. A detailed CV was then recorded at a scan rate of 10 mV s<sup>-1</sup>. The electrode was held in Ar-saturated 0.5 M H<sub>2</sub>SO<sub>4</sub> + 5 mM CuSO<sub>4</sub> at a specific potential for 100 s, followed by an anodic CV scan from that potential to the upper limit at 10 mV s<sup>-1</sup>. The potential was adjusted until bulk Cu deposition appeared in the CV. The ECSA was determined by integrating the Cu UPD peak area according to Equation (1), and the number of  $n$  and TOF were calculated using Equations (2) and (3), respectively.

$$ECSA = 0.42 = \frac{Q_{Cu} \int_{E_1}^{E_2} I(E)d(E)}{v \cdot 0.42} \quad (1)$$

$$n = \frac{Q_{Cu}}{2F} \quad (2)$$

$$TOF = \frac{I}{2Fn} \quad (3)$$

where  $Q_{Cu}$  is the charge obtained from the Cu UPD after subtracting the blank CV recorded in Ar-saturated 0.5 M H<sub>2</sub>SO<sub>4</sub>  $E_1$  and  $E_2$  are the lower and upper voltage limits for Cu UPD, respectively, and  $v$  is the CV scan rate. The conversion factor for Cu deposition is 0.42 mC cm<sup>-2</sup>, and  $F$  is the Faraday constant (96,485 C mol<sup>-1</sup>).

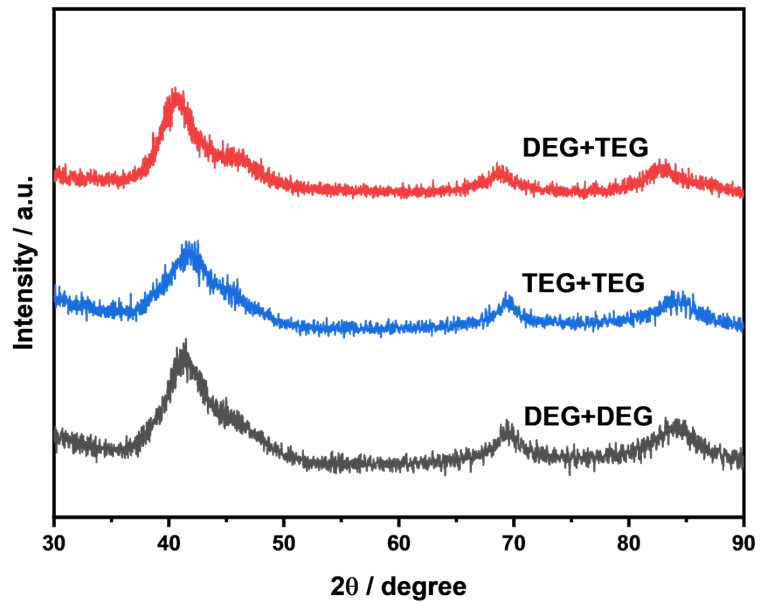


Fig. S1. PXRD patterns of RuCuRhIrPt NPs synthesized using different solvent/reducing agent systems (DEG + TEG, TEG + TEG, and DEG + DEG).

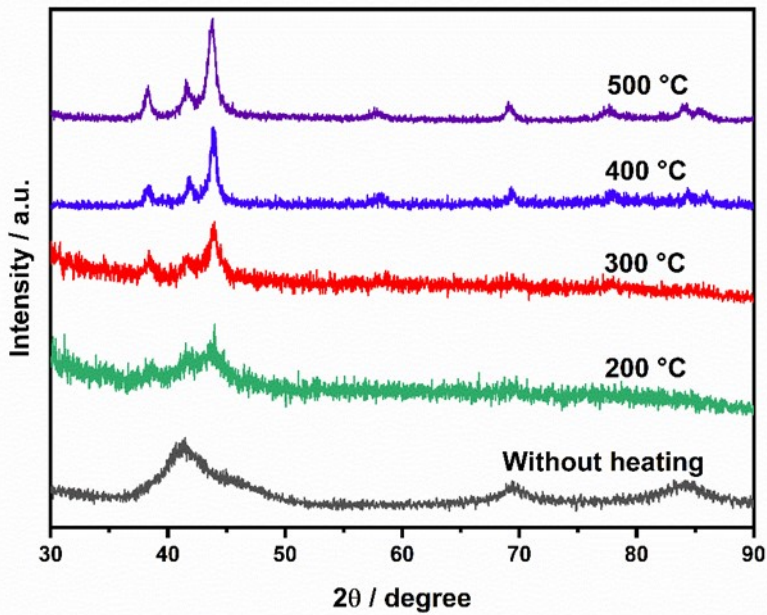


Fig. S2. PXRD patterns of the fcc-RuCuRhIrPt HEA NPs heated at different temperatures for 0.5 h.

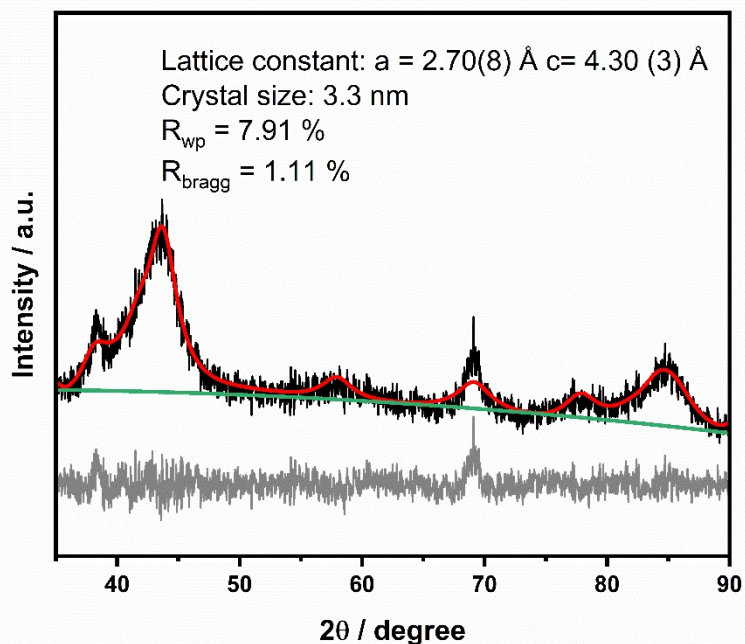


Fig. S3. Rietveld refinement analysis for the Ru NPs. The diffractions patterns are shown as black circles. The calculated patterns are shown as red curves. The difference profile and the background profile are shown as gray and green curves, respectively.

Table S1. ICP-OES results of RuCuRhIrPt HEA NPs.

Samples	Atom (%)				
	Ru	Cu	Rh	Ir	Pt
hcp	70.75	6.58	8.01	7.53	7.14
fcc	69.21	7.34	7.81	8.16	7.48

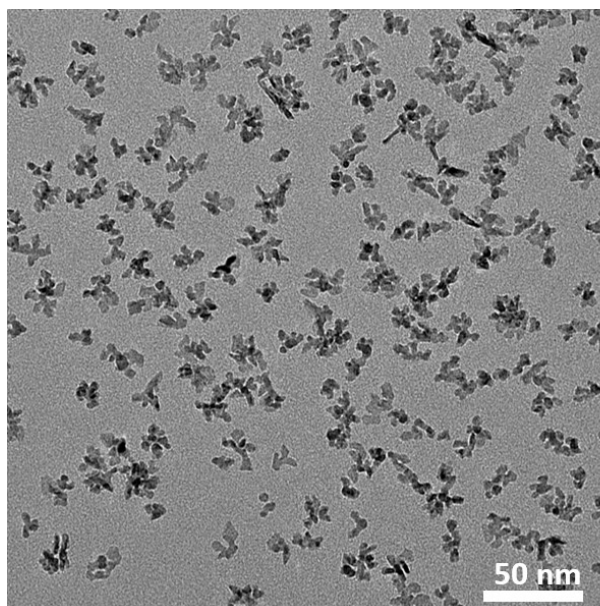


Fig. S4. TEM images of fcc-RuCuRhIrPt without carbon support.

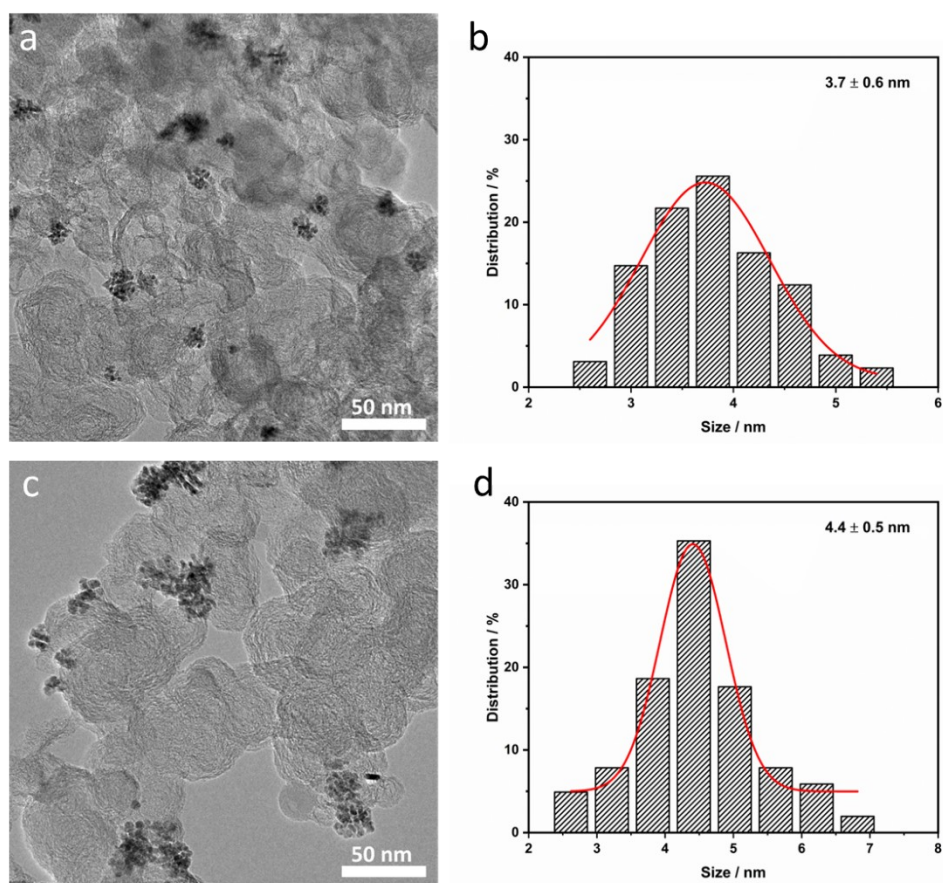


Fig. S5. TEM images of (a) fcc-RuCuRhIrPt/C, and (c) hcp-RuCuRhIrPt/C. Particle size distributions of (b) fcc-RuCuRhIrPt/C and (d) hcp-RuCuRhIrPt/C. The particle size distribution was obtained by measuring 150 particles.

Table S2. Binding energies of Ru 3p, Cu 2p, Rh 3d, Ir 4f and Pt 4f.

Samples	Binding energy (eV)									
	Ru 3p <sub>3/2</sub>	Ru 3p <sub>1/2</sub>	Cu 2p <sub>3/2</sub>	Cu 2p <sub>1/2</sub>	Rh 3d <sub>5/2</sub>	Rh 3d <sub>3/2</sub>	Ir 4f <sub>5/2</sub>	Ir 4f <sub>7/2</sub>	Pt 4f <sub>7/2</sub>	Pt 4f <sub>5/2</sub>
hcp	461.88	484.00	932.59	952.20	307.85	312.67	61.32	64.31	71.98	75.31
fcc	461.88	484.01	932.40	952.16	307.51	312.33	60.91	63.86	71.78	75.07

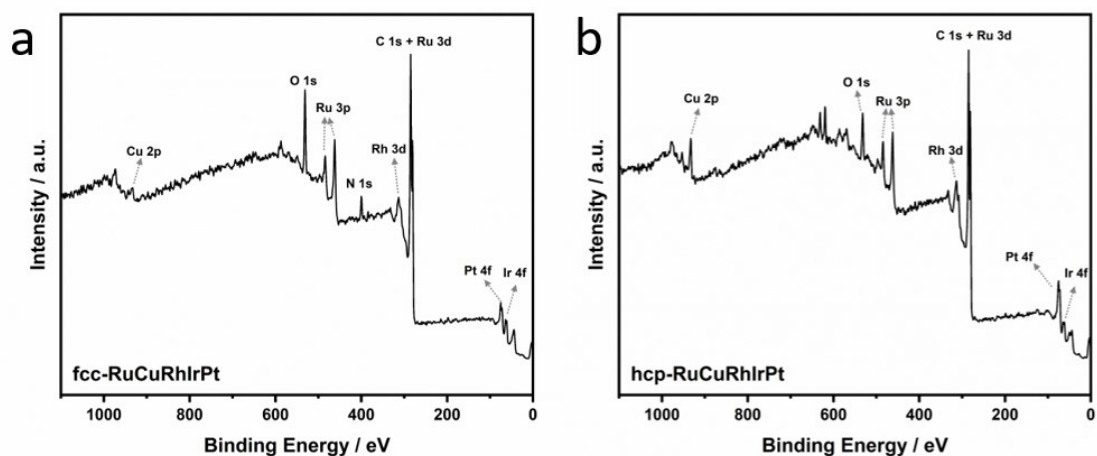


Fig. S6. XPS spectra of (a) fcc- and (b) hcp-RuCuRhIrPt.

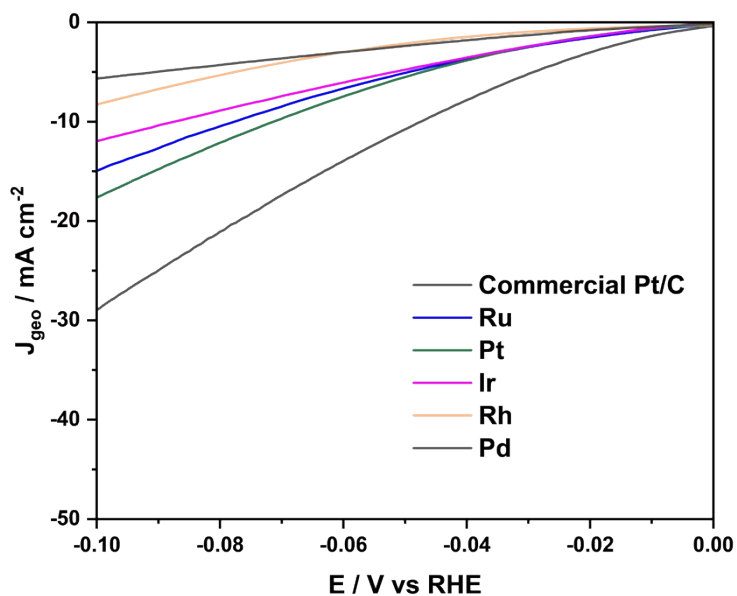


Fig. S7. LSV curves of the commercial fcc-RuCuRhIrPt, Ru, Cu, Rh, Ir and Pt electrocatalysts.

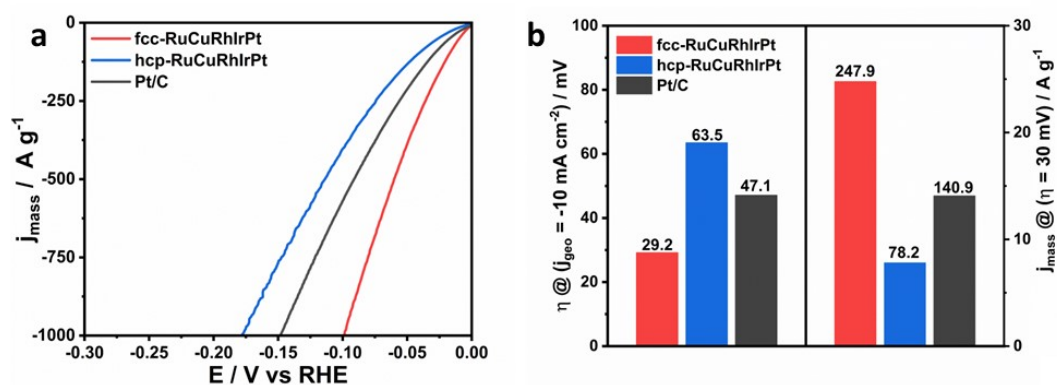


Fig. S8. (a) Mass activity. (b) Comparison of overpotential ( $10 \text{ mA cm}^{-2}$ ) and mass activity ( $\eta = 30 \text{ mV}$ ).

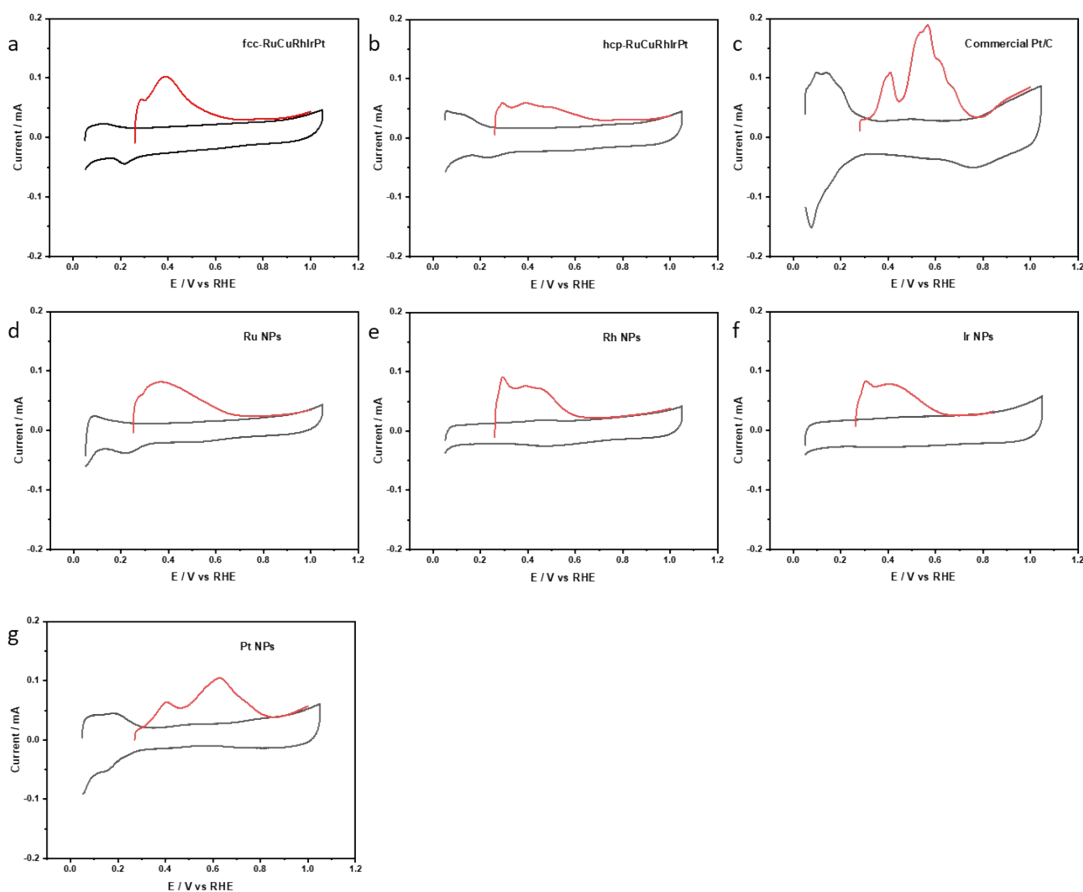


Fig. S9. ECSA measurement of the catalysts. Cu-UPD in  $0.5 \text{ M H}_2\text{SO}_4$  without (black curve) and with  $5 \text{ mM CuSO}_4$  (red curve) on the (a) fcc-RuCuRhIrPt, (b) hcp-RuCuRhIrPt, (c) Commercial Pt/C, (d) Ru NPs, (e) Rh NPs, (f) Ir NPs and (g) Pt NPs.

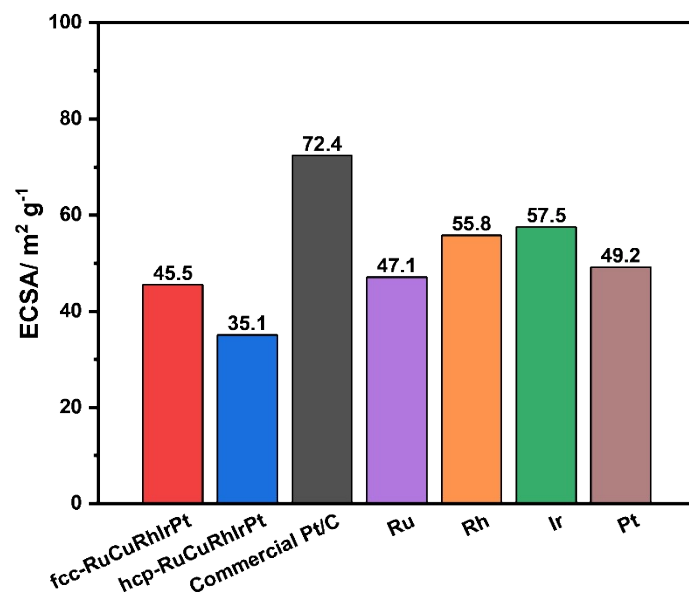


Fig. S10. ECSA of the catalysts.

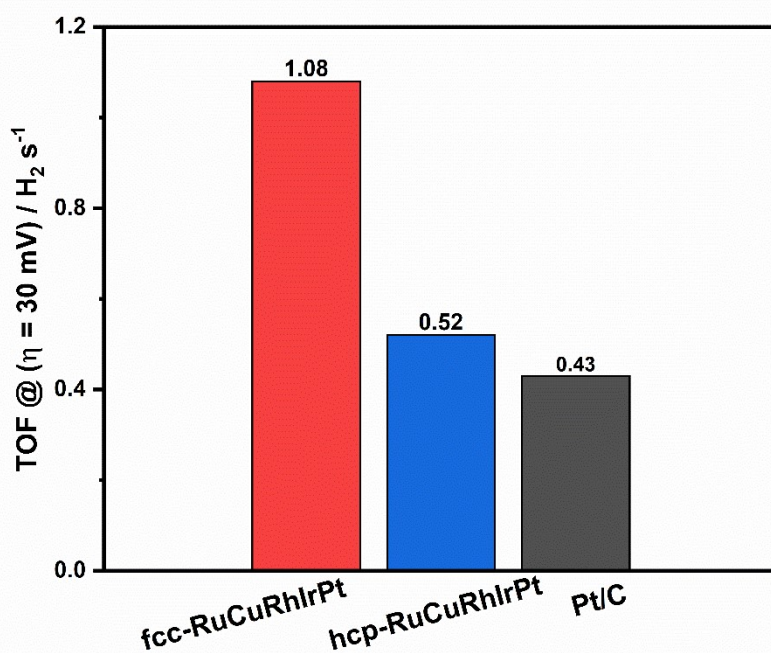


Fig. S11. TOF values (at an  $\eta$  of 30 mV) of RuCuRhIrPt/C and Pt/C.

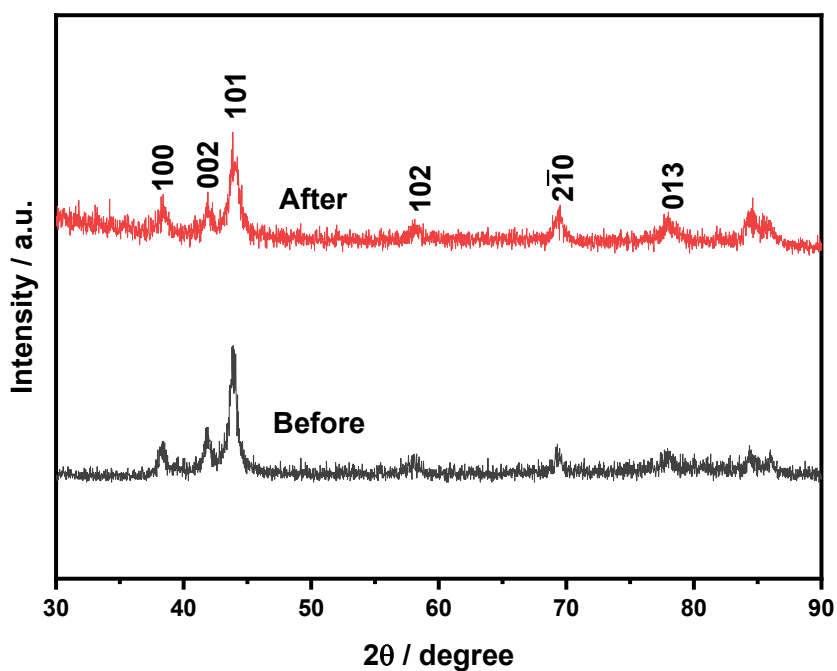


Fig. S12. Structure characterization of hcp-RuCuRhIrPt HEA-NPs before and after the chronoamperometry test.

## References

1. C. L. Green and A. Kucernak, *The Journal of Physical Chemistry B*, 2002, **106**, 11446-11456.
2. M. Łukaszewski, M. Soszko and A. Czerwiński, *International Journal of Electrochemical Science*, 2016, **11**, 4442-4469.
3. M. A. Quiroz, Y. Meas, E. Lamy-Pitara and J. Barbier, *Journal of Electroanalytical Chemistry and Interfacial Electrochemistry*, 1983, **157**, 165-174.